JOURNAL OF CATALYSIS **68**, 423–432 (1981)

Vanadium–Titanium Oxide Catalysts for Oxidation of Butene to Acetic Acid

WILLIAM E. SLINKARD AND PETER B. DEGROOT

Celanese Chemical Company Technical Center, P.O. Box 9077, Corpus Christi, Texas 78408

Received September 8, 1980; revised November 19, 1980

The oxidation of *n*-butenes over V_2O_5–TiO_2 catalysts with air in the presence of steam was found to selectively yield acetic acid and acetaldehyde with some carbon oxides. A number of V_2O_5–TiO_2 catalysts were studied and characterized by surface area, ESCA, and XRD analyses. The catalysts were found to contain V_2O_5, varying amounts of either rutile or anatase TiO_2, and a solid solution of V^{4+} in TiO_2. The relative amounts of these phases present in the catalysts were dependent primarily on the preparation technique. These different V-oxide and Ti-oxide phases present were also related to catalyst performance. The rutile TiO_2-containing catalysts showed higher selectivities to acetic acid and acetaldehyde and lower selectivities to carbon dioxide and formic acid than the comparable anatase TiO_2-containing catalysts. Catalyst activity appeared to be related to the presence of a reduced vanadium moiety incorporated into either the TiO_2 lattice or into partially reduced V_2O_5. Possible causes for these selectivity differences between phases and compositions are discussed as well as the nature of the active catalytic species.

INTRODUCTION

Vanadium oxide-based catalysts in combination with various promoters, e.g., TiO_2, are well known for the selective oxidation of hydrocarbons (*1, 2*), including oxidation of *n*-butenes to acetic acid (*3*). In recent years, studies of V_2O_5–TiO_2 catalysts have concentrated on their use in the oxidation of *o*-xylene to phthalic anhydride (*4–8*) or of butene to butadiene (*9*) or maleic anhydride (*10*). The effects of preparation method and V : Ti ratio on catalyst selectivity and activity (*4–13*) as well as kinetic and mechanistic investigations have been reported (*14–16*). These catalyst studies, as well as others into the solid state chemistry of the V_2O_5–TiO_2 system (*17–20*), have suggested that the active catalytic species is likely a solid solution of V^{4+} in the TiO_2.

In contrast to these investigations of the oxidation of aromatic compounds or of C_4 hydrocarbons to butadiene or maleic anhydride, few catalyst studies have been reported on the oxidation of butenes to acetic acid (*21–23*) outside of the patent literature. As yet, no study of this system with detailed catalyst characterization data has been reported. In light of the expected increased availability and possible importance of butenes for the production of petrochemicals such as acetic acid (*24*), we have investigated the oxidation of butenes to acetic acid with V_2O_5–TiO_2 catalysts.

EXPERIMENTAL

Catalyst Testing Apparatus and Procedure

Catalysts were tested in a fixed bed, U-shaped tubular stainless-steel microreactor constructed with a 1.6-mm-o.d. thermowell running down the center of the catalyst-containing leg of the reactor. A thermocouple (0.8 mm o.d.) could be moved up and down the length of the catalyst bed for temperature profiling. The reactor was about 60 cm in height with the catalyst-containing section having an i.d. of about 12 mm.

The usual catalyst charge was 5 cm^3 of $-20 + 30$ mesh material physically mixed with 5 cm^3 of 24 grit Norton silicon carbide.

0021-9517/81/040423-10$02.00/0

This dilution of the catalyst was necessary to control the temperature in the catalyst bed and prevent excessive exotherms. Even so, it was not possible to maintain isothermal operation and, consequently, reliable kinetic data could not be obtained.

All experiments were conducted at atmospheric pressure. The feed gas consisted of butene, air, and steam in a volume ratio of about 1 : 20 : 20. The *n*-butene mixture used had a composition of about 50% 1-butene and 50% 2-butene. Flow rates were adjusted to obtain a contact time of about 5 sec (NTP). Feed and vent gas streams, after condensible liquids were recovered in a chilled catchpot, were analyzed on-line by gas chromatography. Components analyzed included carbon monoxide, carbon dioxide, oxygen, nitrogen, 1-butene, 2-butene, 1,3-butadiene, and any acetaldehyde and acetone not condensed with the liquid product. The liquid product was collected after each experiment. Liquid components analyzed included acetic acid, acetaldehyde, acetone, propionic acid, butyric acid, maleic acid, methyl ethyl ketone, 1- and 2-butanol, acrylic acid, acrolein, methacrylic acid, and methacrolein. Formaldehyde was analyzed by addition of sodium sulfite followed by sulfuric acid titration. Formic acid analysis was done by lead tetraacetate treatment followed by sodium thiosulfate titration. Carbon and oxygen accountabilities were at least 100 ± 10% and generally ±5% for all experiments.

The terms "conversion" and "selectivity" as used in this paper are defined in the following manner. Conversion is defined as mole percent conversion and is calculated by multiplying the moles of reactant consumed times 100 and dividing by the moles of reactant fed. Selectivity to a particular product is defined as mole percent selectivity on a carbon-accounted-for basis and is calculated by multiplying the number of moles of carbon atoms in a particular product obtained times 100 and dividing by the number of moles of carbon atoms in all the products recovered.

Catalyst Preparation

The vanadium–titanium oxide catalysts were prepared by one of four general procedures involving either precipitation of the oxides from acid solution with base or forming a solid mixture of vanadyl oxalate either with titanium oxalate or hydrated titania. In each procedure below, the recovered solid was calcined in air for about 16 hr.

(A) Aqueous solutions of the appropriate quantities of vanadyl oxalate and titanium oxalate were combined and the water removed on a rotary evaporator.

(B) Hydrated titania, freshly precipitated with ammonium hydroxide from a hydrochloric acid solution of $TiCl_4$, was combined with the appropriate amount of vanadyl oxalate solution to form a slurry and the slurry spray dried.

(C) The mixed oxides were precipitated from a hydrochloric acid solution in one step with ammonium hydroxide at a pH of about 6.

(D) The mixed oxides were precipitated from acid solution with base as in Procedure C, but in two steps. Precipitation was first carried out at a pH of about 2 followed by adjustment of the reaction mixture with ammonium hydroxide to a final pH of about 5.7. The recovered brown precipitate was either calcined directly (D.1) or treated with H_2O_2 to form a bright yellow solid and then calcined (D.2).

The catalysts prepared, preparation details, and the resulting surface area and relative rutile/anatase TiO_2 phase compositions are summarized in Table 1. The titania catalyst was prepared as in Procedure C but without vanadium present. The vanadium oxide catalyst was prepared as in Procedure A without titanium present but first calcined in a restricted, stagnant atmosphere (A.1) and then calcined again in air (A.2).

For convenience, mixed vanadium–titanium oxide catalysts will be designated by a number giving the Ti/V ratio followed by a

TABLE 1

Characterization and Preparation of Vanadium, Titanium, and Vanadium/Titanium Oxide Catalysts

Catalyst composition	Preparation technique	Calcination temp. (°C)	Surface area (m^2/g)	Approximate TiO_2 composition	
				% Rutile	% Anatase
$VTiO_x$	B	520	2.5	100	0
$VTiO_x$	A	450	30	95	5
$VTiO_x$	C	420	9.0	85	15
$VTiO_x$	D.1	400	35	10	90
$VTiO_x$	D.2	400	40	0	100
Ti_4VO_x	B	500	15	60	40
Ti_4VO_x	D.1	500	94	0	100
TiO_2	C	450	75	0	100
V_2O_x	A.1	400	33	—	—
V_2O_5	A.2	400	15	—	—

letter designating the preparation procedure above. For example, a $VTiO_x$ catalyst prepared according to Procedure C would be 1C.

Catalyst Characterization

Surface area. Surface areas were measured by N_2 adsorption in a Micromeritics Model 2200 High Speed Surface Area Analyzer.

X-ray diffraction. Powder X-ray diffraction (XRD) data were obtained with a Norelco X-ray diffractometer interfaced to a Tracor-Northern NS-880 energy-dispersive X-ray data system. High resolution data were obtained in digital form at 0.01° 2θ increments. Lower resolution XRD data were also obtained as analog strip-chart records. CuK_α radiation was used along with a graphite crystal monochromator. KCl was added to the sample as an internal standard.

Average crystallite sizes were obtained from diffraction line widths by the method of Debye and Scherrer (*25*). The lines used were the {110} for V_2O_5 and TiO_2–rutile, and {101} for TiO_2–anatase.

Relative fractions of rutile and anatase were calculated from the ratio of the peak height or area of the rutile {110} diffraction line to the peak height or area of the anatase {101} line (*19*).

The amount of VO_2 incorporated into the TiO_2 lattice was calculated from the observed change in selected *d*-spacings relative to pure rutile or anatase. One or more of the following diffraction lines were used for this purpose: Rutile—{110}, {101}, {200}, {210}. Anatase—{101}, {200}. The *d*-spacings for these lines in the pure phases were calculated from lattice dimensions measured by the National Bureau of Standards (*26, 27*). The expected *d*-spacings for rutile incorporating varying amounts of VO_2 were calculated from the data of Marinder and Magneli (*28*), assuming a linear relationship. Since corresponding experimental data for anatase were not available, the assumption was made that the relative change in lattice dimensions with VO_2 content was the same for anatase as for rutile.

X-ray photoelectron spectroscopy. XPS or ESCA (electron spectroscopy for chemical analysis) was done using a Physical Electronics Model 550 Auger/ESCA system. MgK_α radiation was used. Binding energies were measured relative to C 1s = 285.0 eV. Ion sputtering experiments were done using 5 kV Ar^+ ions.

Catalyst samples were prepared for analysis by grinding to ~100 mesh and pressing the resulting powder onto the surface of indium foil. Sample preparation took place under ambient conditions.

RESULTS AND DISCUSSION

Catalyst Characterization—XRD

The results from high resolution XRD analysis (Table 2) reveal that these V_2O_5–TiO_2 catalysts contain V_2O_5 and varying amounts of either rutile or anatase TiO_2 depending on the method of preparation. A two-step precipitation of hydrated V_2O_5–TiO_2 (Procedure D) leads to high concentrations of anatase in the catalyst and low concentrations of rutile, whereas a one-step precipitation (Procedure C) leads to a high rutile content catalyst. The use of vanadyl oxalate either with hydrated Ti oxide or Ti oxalate also leads to primarily rutile-containing catalysts. Without vanadium present, however, only anatase is formed by any of the preparative techniques at normal calcination temperatures of 400–500°C. Apparently vanadium, under these conditions, catalyzes the transformation of the anatase form of TiO_2 to rutile, as previously reported (*10*).

Both the amount of rutile and the fraction of VO_2 incorporated into the rutile phase increase upon catalyst use. This is indicated both by *d*-spacing changes and by a decrease in the peak area of the remaining V_2O_5. The fraction of VO_2 incorporated into anatase, on the other hand, decreases with use. One predominantly rutile-containing catalyst (1A) incorporates much more VO_2 in the TiO_2 phase than either of the other two mostly rutile catalysts (1B and 1C), or any of the predominantly anatase-containing materials.

Average crystallite sizes of both rutile and anatase in most of the V:Ti catalysts are similar (Table 2). Incorporation of VO_2 into the TiO_2 lattice does not seem to affect crystallite size. The crystallite size of the V_2O_5 present ranges from 35 to >150 nm. One of the 4:1 Ti:V catalysts (4B) contains both rutile and anatase. The rutile crystallite size is similar to that of the 1:1 catalysts, while the anatase crystallite size is considerably larger.

Catalyst Surface Characterization—ESCA

ESCA results on catalysts are given in Table 3. Vanadium $2p_{3/2}$ peak positions in all cases are indicative of V^{5+}. The rather narrow peak width of ~1.5 eV, observed in all cases except that of the 95% rutile

TABLE 2

Characteristics of V/Ti Oxide Catalysts from High Resolution XRD Data

Catalyst	State	% TiO_2 as rutile	x in $(TiO_2)_{1-x} \cdot (VO_2)_x$		Average crystallite size (nm)		
			Rutile phase	Anatase phase	Rutile	Anatase	V_2O_5
1A	Unused	95	0.24	—	22	—	64
1A	Used	95	0.40	—	25	—	
			0.36	—	21	—	69
1B	Used	100	0.16	—	49	—	70
1C	Unused	74	0.04	0.12	29	20	49
		79	0.01	0.10	30	19	51
1C	Used	85	0.14	0.07	26	19	35
1D.1	Unused	10	—	0.09	—	22	71
			—	0.07	—	24	>150
1D.1	Used	10	—	0.04	—	25	70
1D.2	Unused	0	—	0.09	—	26	>150
4B	Used	61	0.07	0.01	29	57	76
4D.1	Unused	0	—	0.05	—	10	—

TABLE 3

ESCA Binding Energies, Peak Widths, and Surface V/Ti Ratios

Catalyst	State	$V2p_{3/2}$		$Ti2p_{3/2}$		O ls		V/Ti atomic ratio
		B.E. (eV)[a]	Width $\frac{1}{2}$ max (eV)	B.E. (eV)	Width $\frac{1}{2}$ max (eV)	B.E. (eV)	Width $\frac{1}{2}$ max (eV)	
1A	Unused	517.3	2.2	458.6	1.3	530.0	1.5	0.72
1A	Used	517.2	1.9	458.8	1.4	530.2	1.5	0.98
1C	Unused	516.8	1.6	458.1	1.4	529.5	1.7	1.3
1C	Used	517.1	1.6			529.8	1.7	
1D.2	Unused	516.7	1.6	458.2	1.3	529.6	1.7	1.2
1D.1	Unused	517.3	1.5	458.8	1.3	530.1	1.6	0.76
1D.1	Used	517.2	1.5	458.8	1.4	530.1	1.5	0.75
4D.1	Unused	517.0	1.8	458.5	1.5	529.6	1.6	0.59
V_2O_5	—	517.4	1.5	—	—	530.2	1.5	—
TiO_2 (anatase)	—	—	—	458.7	1.3	529.9	1.6	—
TiO_2 (rutile)	—	—	—	458.9	1.4	530.2	1.6	—

[a] Binding energy scale corrected to C ls = 285.0 eV.

VTiO$_x$ catalyst (1A), is also similar to that observed for V_2O_5. Ti2p$_{3/2}$ peaks in all cases would be consistent with either rutile or anatase. Likewise, the O 1s peak positions and widths for TiO_2 phases and for V_2O_5 are not distinguishable from each other or from the position observed in all of the catalysts.

These differences among catalysts revealed by ESCA are minimal. The lower-valent vanadium oxides are well known for being extremely sensitive to surface oxidation on exposure to air or moisture. It is not surprising, then, that all the catalyst surface vanadium appears to be in the +5 oxidation state. The situation is further complicated by the presence of a large amount of excess V_2O_5 in addition to any vanadium incorporated into the titanium oxide.

Only the catalyst (1A) containing a fairly large (25–35%) amount of VO_2 in the rutile phase exhibits a broad V2p$_{3/2}$ peak. This may be due to contributions from both "free" V_2O_5 and $VO_2 \cdot TiO_2$. VO_2, either free or incorporated into rutile or anatase, has a broader 2p$_{3/2}$ photoelectron peak, which is also shifted to about 1 eV lower binding energy than that of V_2O_5 (*29–31*). Scans at the highest resolution of the instrument (FWHM of Au4f$_{7/2}$ = 0.7 eV) did not indicate any multiple peak structure.

The surface V/Ti atomic ratios have also been calculated from V2p$_{3/2}$ peak areas and published sensitivity factors (*29*). They are included in Table 3. In the VTiO$_x$ catalysts, the values range from about 30% below to about 30% above the bulk average 1 : 1 ratio. In the one Ti$_4$VO$_x$ catalyst examined by ESCA, the surface V/Ti ratio is about twice the bulk average ratio.

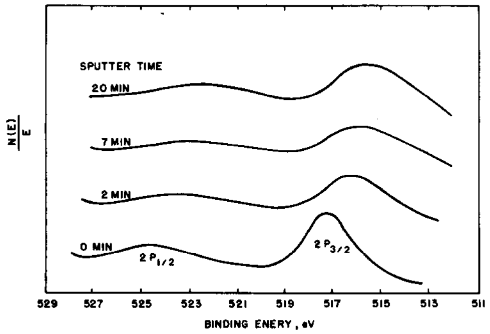

FIG. 1. Effect of sputter-etching with 5 keV Ar$^+$ ions on V2p$_{3/2}$ photoelectron spectrum of catalyst 1A.

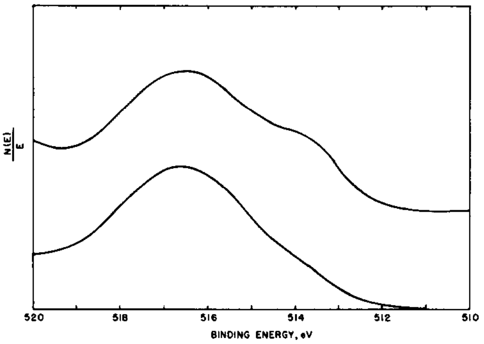

FIG. 2. Effect of sputter-etching for 20 min with 5 keV Ar$^+$ ions on the V2p$_{3/2}$ photoelectron peak. Upper curve, catalyst 1A. Lower curve, physical mixture of V_2O_5 and rutile TiO_2.

Ion sputtering experiments were also performed in conjunction with ESCA experiments. All the catalysts behaved similarly. As shown in Fig. 1, vanadium was rapidly reduced to lower oxidation states. Some of it was reduced all the way to the metal. In contrast, sputtering either pure V_2O_5 or a physical mixture of V_2O_5 and TiO_2 (Fig. 2) produced reduction of V^{5+} to a lesser extent.

Catalyst Performance

The oxidation of either 1-butene or a mixture of *n*-butenes over V_2O_5–TiO_2 with air in the presence of steam yielded primarily acetic acid, acetaldehyde, and carbon oxides with only minor amounts of other organic by-products. Results are summarized in Table 4. Acetyl selectivity (sum of acetic acid plus acetaldehyde selectivities) increased from 52 to 54% with VTiO$_x$ catalysts (1D.1 and 1D.2) containing 90–100% anatase to 58–62% selectivity with 85–100% rutile (1A, 1B, 1C). In addition, the high anatase-containing catalysts produced significantly more formic acid than the high

TABLE 4

Oxidation of Mixed *n*-Butenes over Vanadium/Titanium, Vanadium, and Titanium Oxide Catalysts

Catalyst	Temp. (°C)[a]	Butene[b] conv. %	Selectivity (%)[c]				
			Acetic acid	Acetaldehyde	C oxides	Formic acid	Others[d]
1A	230	97	51	9.3	35	1.4	3.2
1B	245	88	47	15	30	2.0	7.9
1C	250	95	48	10	38	1.4	2.7
1D.1	215	94	41	11	38	5.1	5.5
1D.2	200	92	39	15	34	7.5	5.0
4B	205	35	43	31	17	1.5	6.2
4D.1	180	34	43	23	20	7.8	5.6
V_2O_x	220	60	40	25	19	4.3	10
V_2O_5	280	59	27	20	30	3.0	20
TiO_2	300	40	12	5.4	72	0.5	10

[a] Shell temperature. Catalyst peak temperatures were generally about 5–10°C higher at butene conversions above 50% and less than 5°C higher at lower conversions.

[b] Butene conversion = moles of butene in − moles of butene out/moles of butene in × 100%.

[c] Carbon selectivity on a carbon accounted for basis, e.g., acetic acid selectivity = moles of carbon in acetic acid analyzed/moles of carbon in all products analyzed × 100%.

[d] Butadiene, acetone, propionic acid, maleic acid, acylic acid, and formaldehyde.

rutile content catalysts (5–7% selectivity versus 1–2%). The Ti_4VO_x catalysts showed the same selectivity trends as the $VTiO_x$ catalysts.

Product selectivity as a function of butene conversion was studied with two $VTiO_x$ catalysts (1A and 1D.1) containing either mostly rutile or mostly anatase TiO_2 (Figs. 3–5). As shown, acetyl selectivity was considerably higher at low butene conversions than at high conversions for both catalysts. The rutile-containing $VTiO_x$ catalyst gave higher acetic acid selectivities than the anatase-containing catalyst over the entire range of butene conversions (35–95%). Acetaldehyde selectivities were also higher for the rutile than the anatase-containing catalyst at butene conversions below 90%.

CO_2 was consistently higher for the anatase-containing $VTiO_x$ catalyst (1D.1) than for the predominantly rutile catalyst (1A) up to about 90% butene conversion, whereas CO selectivity was nearly identical for both catalysts. The increase in CO_2 selectivity appeared to parallel the decrease in acetic acid selectivity, while CO and acetaldehyde appeared to be inversely related.

Both TiO_2 and V_2O_5 were tested individually as oxidation catalysts for 1-butene and mixed *n*-butenes. In addition, a V oxide catalyst, V_2O_x, containing a mixture of V oxides (V_2O_5, V_3O_5, V_2O_4, V_2O_3, etc.) was also studied. Surprisingly, the V_2O_x catalyst was as active and selective as the V_2O_5–TiO_2 catalysts. Acetyl selectivity was 65% at 60% butene conversion for V_2O_x compared with 62% selectivity at 59% con-

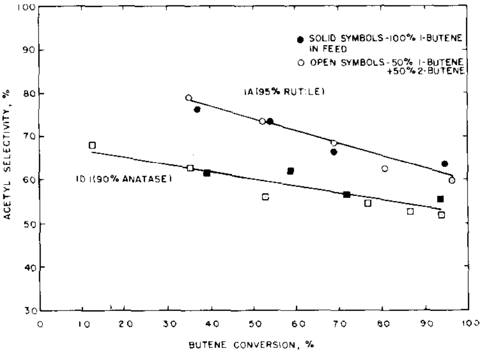

FIG. 3. Effect of TiO_2 phase in $VTiO_x$ on acetyl selectivity from *n*-butene oxidation.

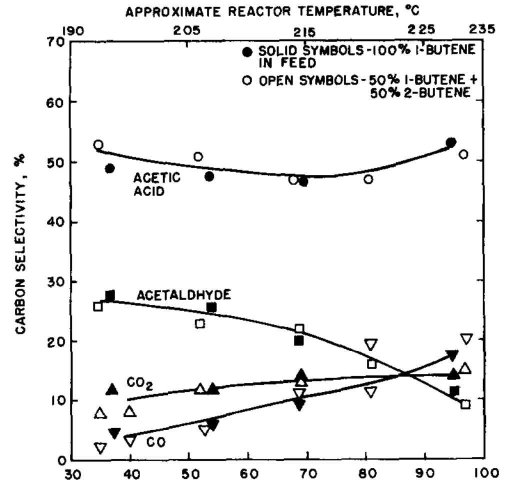

FIG. 4. Effect of butene conversion on product selectivity using catalyst 1A (95% rutile).

version for $VTiO_x$ (1D.1). Stoichiometric V_2O_5, on the other hand, was much less active and selective than either V_2O_x or $VTiO_x$. TiO_2 was nearly inactive and produced mainly carbon oxides.

Catalyst Performance—Isomerization

Conceivably, isomerization of butene isomers could be important for a selective catalyst, if isomerization was slow compared to oxidation. However, for V_2O_5–TiO_2 catalysts, this is not the case. Product selectivities were approximately the same regardless of the mix of butene isomers in the feed gas. Moreover, as shown in Fig. 6, essentially equilibrium concentrations of *n*-butene isomers were observed for the unconverted *n*-butenes in the vent gas, even at low conversions, over both $VTiO_x$ catalysts (1A and 1D.1) as well as V_2O_x and V_2O_5. TiO_2 (100% anatase) and SiC showed littled isomerization activity. Clearly, vanadium oxide is responsible for the high isomerization activity of V_2O_5–TiO_2 catalysts, consistent with the results of Ai (*9*).

Nature of the Active Catalytic Species

From the present results, it appears that a lower valent vanadium species is necessary for a selective catalyst with good activity for the oxidation of butenes to acetic acid. This might be either V^{4+} incorporated into the TiO_2 lattice or V^{4+} or other low valent species in the V_2O_5 also present, since partially reduced V_2O_5 alone was observed to be a good catalyst for the reaction. The decrease in TiO_2 lattice spacing observed certainly indicates substitution of the smaller V^{4+} ions for Ti^{4+} in the lattice to some extent in almost all catalysts. ESR evidence coupled with ESCA has also confirmed that vanadium (at the ~1% level) incorporated into TiO_2 is all in the +4 oxidation state (*20*).

However, the substitutional V^{4+} in the TiO_2 lattice is not solely responsible for the observed catalytic behavior. Both $VTiO_x$ and V_2O_x had comparable activity and selectivity. Moreover, the 100% rutile catalyst (1B), the 95% rutile catalyst (1A), and the 85% rutile catalyst (1C) also had very different V^{4+} contents but comparable performance. Possibly only a surface lower-valent vanadium species is catalytically important.

Catalyst Performance—Effect of Rutile or Anatase TiO_2

The results show clearly that the rutile form of TiO_2 combined with V_2O_5 is preferred over V_2O_5 plus anatase for a selective catalyst. V_2O_5–TiO_2 catalysts con-

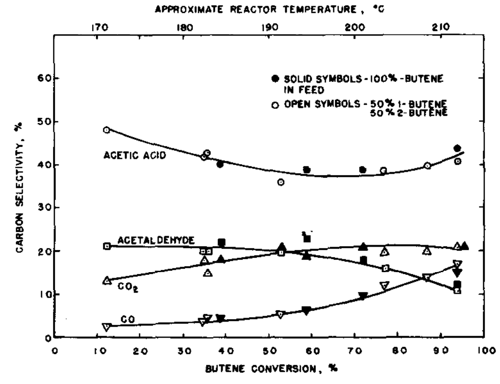

FIG. 5. Effect of butene conversion on product selectivity using catalyst 1D.1 (90% anatase).

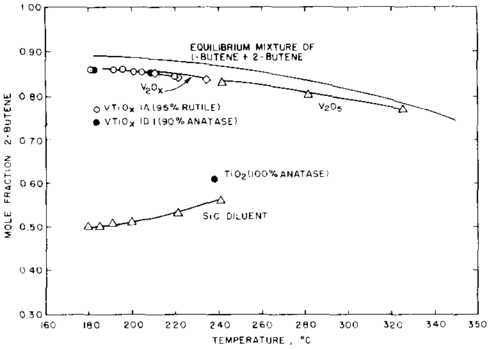

FIG. 6. Mole fraction of 2-butene in unreacted butene in vent gas from low-conversion oxidation over vanadium and titanium oxides, catalysts, and SiC catalyst diluent. The feed is an equimolar mixture of 1-butene and 2-butene. Equilibrium values at various temperatures were taken from Ref. (*35*).

taining more than 50% rutile have been claimed previously to give higher acetic acid yields than catalysts with lower amounts of rutile (*32*).

The role of TiO_2 in producing these differences in performance may be due to different types of V^{4+} being incorporated into the titania lattice, perhaps substitutional (rutile) vs interstitial (anatase), as suggested by Meriandeau and Vedrine (*20*). On the other hand, the higher CO_2 and lower acetyl selectivities for anatase compared to rutile $VTiO_x$ catalysts suggest that anatase TiO_2 may just be more active for the decomposition of the acetic acid or acetaldehyde product. Indeed, the rate of photodecomposition of acetic acid (in solution) was found to be much faster on anatase than on rutile both in the presence and absence of oxygen (*33*).

Mechanism of Acetic Acid Formation

The best-developed mechanism proposed to date for the oxidation of butenes to acetic acid suggests that acetic acid is formed in a series of reactions from an alcohol intermediate (*22*, *23*, *34*). The proposed initial reaction of *n*-butene is hydration to *sec*-butanol followed by oxydehydrogenation to methyl ethyl ketone. Oxidative C–C bond scission then forms equimolar quantities of acetic acid and acetaldehyde. The acetaldehyde may then be further oxidized to produce additional acetic acid.

Our results are consistent with this oxyhydrative scission mechanism. In most of our experiments, the acetaldehyde–acetic acid ratio increases with decreasing butene conversion, but is never more than one. This suggests that acetic acid is produced in a reaction pathway parallel to acetaldehyde formation as well as consecutively from acetaldehyde.

A lower-valent vanadium species may be important to this mechanism. As in other selective oxidations, a redox mechanism involving lattice oxygen has been suggested (*10*, *34*) for oxidative scission. In this regard, increased reducibility or lattice oxygen mobility in the catalyst would imply a more facile oxydehydration or oxidation of the adsorbed species. Such increased reducibility has been observed for both the $TiVO_x$ and V_2O_5 phases present in vanadium–titanium oxide catalysts, and is ascribed either to defect formation or weakened Ti–O bonds (*7*, *10*, *19*). Clearly further investigation is needed to define the mechanistic step(s) in which V^{4+} is important, and in what phase(s) (V_2O_5 or $VTiO_x$) the catalytic species resides.

CONCLUSIONS

A lower valent vanadium species is needed for a selective, active catalyst for the oxidation of *n*-butene to acetic acid and acetaldehyde.

This active species can be produced by partially reducing V_2O_5 or by preparing V/Ti oxides in which V^{4+} is incorporated into the TiO_2 lattice. The function of TiO_2 in the V_2O_5–TiO_2 catalysts may be to serve as a host for the V^{4+} moiety and to stabilize it against oxidation to the less active V^{5+} state.

Identification of the active species in V_2O_5–TiO_2 catalysts is complicated by the presence of V_2O_5 along with the V/TiO_2 phase. The ease of reduction of this V_2O_5

observed in ion-sputtering experiments suggests that under reaction, partial reduction of this phase may also occur, generating another active reduced vanadium species.

Catalysts containing rutile TiO_2 have higher selectivities to acetic acid and acetaldehyde than anatase-containing catalysts. Possible reasons for this are higher concentration of V^{4+} in the rutile lattice, different position of V^{4+} in the rutile lattice (substitutional versus interstitial), and higher stability of products on rutile than on anatase surfaces.

REFERENCES

1. Hucknall, D., "Selective Oxidation of Hydrocarbons." Academic Press, New York, 1974.
2. van de Wiele, K., and van den Berg, P. *in* "Comprehensive Chemical Kinetics" (C. Bamford and C. Tipper, Eds.), Vol. 20, pp. 123–262. Elsevier, New York, 1978.
3. Brockhaus, R., *Chem. Ing. Tech.* **36,** 1039 (1966).
4. Grabowski, R., Grzybowska, B., Haber, J., and Sloczynski, J., *React. Kinet. Catal. Lett.* **2,** 81 (1975).
5. Yabrov, A., Ismailov, E., Boreskov, G., Ivanov, A., and Anufrienko, V., *React. Kinet. Catal. Lett.* **3,** 237 (1975).
6. Cole, D., Cullis, C., and Hucknall, D., *J. Chem. Soc., Faraday Trans.* **72,** 2185 (1976).
7. Adamska, B., Brückman, K., and Grzybowska, B., *Bull Acad. Polonaise Sci.* **24,** 159 (1978).
8. Dyrek, K., Serwicka, F., and Grzybowska, B., *React. Kinet. Catal. Lett.* **10,** 93 (1979).
9. Ai, M., *Bull. Chem. Soc. Japan* **49,** 1328 (1976).
10. Bond, G., and Sárkány, A., *J. Catal.* **57,** 476 (1979).
11. Fabuss, B., "Actes Zeme Congress Int. Catalyst," pp. 2561-2567, Edition Techniq., Paris, 1961.
12. Vanhove, D., and Blanchard, M., *Bull. Soc. Chem. France* 3291 (1971).
13. Blanchard, M., Longuet, G., Rivasseau, J., and Delgrange, J., *Bull Chem. Soc. France* 3071 (1972).
14. Blanchard, M., and Longuet, G., *Kinet. Katal.* **14,** 30 (1973).
15. Vanhove, D., and Blanchard, M., *J. Catal.* **36,** 6 (1975).
16. Vanhove, D., and Blanchard, M., *J. Chim. Phys., Phys. Chim. Biol.* **73,** 51 (1976).
17. Rüdorff, V., Walter, G., and Stadler, J., *Z. Anorg. Allgem. Chem.* **297,** 1 (1958).
18. Pyechotta, V., Ebert, I., and Scheve, J., *Z. Anorg. Allgem. Chem.* **368,** 10 (1969).
19. Yoshida, A., Murakami, T., and Tarama, K., *Bull. Inst. Chem. Res. Kyoto Univ.* **51,** 195 (1973).
20. Mériandeau, P., and Vedrine, J., *Nouv. J. Chem.* **2,** 133 (1979).
21. Kaneko, K., Koyama, T., and Wada, S., *Bull. Japan Petrol. Inst.* **18,** 17 (1974).
22. Yamashita, T., Ninagawa, S., and Kato, T., *Bull. Japan Petrol. Inst.* **18,** 167 (1976).
23. Seiyama, T., Nita, K., Marhara, T., Yamaze, N., and Takita, Y., *J. Catal.* **49,** 164 (1977).
24. Guercio, V., *Oil Gas J.* February 21, 1977, pp. 68–71.
25. Klug, H., and Alexander, L., "X-ray Diffraction Procedures." John Wiley, New York, 1954.
26. Swanson, H., *et al.*, National Bureau of Standards, Monograph 25, Section 7, 82, 1969.
27. Swanson, H., *et al.*, National Bureau of Standards, Monograph 25, Section 7, 83, 1969.
28. Marinder, B., and Magneli, A., *Acta Chem. Scand.* **11,** 1635 (1957).
29. Wagner, C., *et al.*, "Handbook of X-ray Photoelectron Spectroscopy." Perkin-Elmer Corporation, Physical Electronics Division, Eden Prairie, Minn., 1979.
30. Sawatsky, G., and Antonides, E., *J. Phys. (Paris), Colloq.* 1976, 117.
31. Blaauw, C., *et al.*, *J. Phys. C: Solid State Phys.* **8,** 459 (1975).
32. Mizukami, T., Akahane, T., and Fuchigami, Y., U.S. 3,917,682, November 4, 1975. (Assigned to Kuraray Company.)
33. Kraeutler, P., and Bard, A. J., *J. Amer. Chem. Soc.* **100,** 5985 (1978).
34. Takita, Y., Nita, K., Maehara, T., Yamazoe, N., and Seiyama, T., *J. Catal.* **50,** 364 (1977).
35. Voge, H., and May, N., *J. Amer. Chem. Soc.* **68,** 550 (1946).